Pharmaceutical Research, Vol. 23, No. 5, May 2006 (© 2006)
DOI: 10.1007/s11095-006-9903-7

Research Paper

Characterization of Complexes Between Naftifine and Cyclodextrins in Solution and in the Solid State

Maite Uzqueda,[1] Carmen Martín,[1] Arantza Zornoza,[1] Miguel Sánchez,[1] María Cristina Martínez-Ohárriz,[1] and Itziar Vélaz[1,2]

Received September 23, 2005; accepted December 29, 2005

Abstract. Naftifine (NF) is an antifungal drug poorly soluble in basic aqueous solutions. Complexation with cyclodextrins (CDs) improves the physicochemical characteristics of many drugs. The aim of this work is to characterize the interactions between NF and α-CD, β-CD, hydroxypropylβ-CD, methylβ-CD, and γ-CD. The studies have been developed in pH 12 aqueous solutions at 25°C and in the solid state. The apparent stability constants of the complexes have been determined from phase-solubility diagrams. In the solid state, crystalline and amorphous complexes have been characterized using X-ray diffraction patterns, thermal analysis, and Fourier transform infrared spectroscopy. The solubility of NF improves with all the CDs studied, with the exception of α-CD. Different types of diagrams have been found depending on the CD used. The interaction between NF and hydroxypropylβ-CD is stronger than that with β-CD due to the specific properties of the substituents. The coevaporation method can be said the best method in preparing the solid complexes, except for NF–α-CD; again, there is no evidence of complexation. Furthermore, the presence of different types of CD structures upon complexation (i.e., cage or channel) has been discussed. Dissolution rate studies have been performed, and a positive influence of complexation in the solid state has been observed.

KEY WORDS: cyclodextrins; dissolution rate; naftifine; solid state; solubility diagrams.

INTRODUCTION

Naftifine (NF) (*E*)-*N*-methyl-*N*-(1-naphthyl-methyl)-3-phenyl-2-propen-1-amine-hydrochloride (Fig. 1) is an allylamine derivative and represents a new chemical group of antifungal compounds. NF action consists in inhibiting squalene epoxidation, an earlier stage in the ergosterol pathway, by interacting with the squalene epoxidase (1). It is active against a wide range of pathogenic fungi both *in vivo* and *in vitro*. In various clinical studies, NF has shown high efficacy as a topical agent against various types of dermatomycoses. Biochemical studies have shown a specific inhibitory effect in sterol biosynthesis of *Candida albicans*, *Candida parapsilissis*, and *Trichophyton mentagrophytes* (2).

Cyclodextrins (CDs) are cyclic oligosaccharides containing six (α-CD), seven (β-CD), and eight (γ-CD) or more α-(1,4)-linked glucose units. The most important structural feature of these compounds is their toroidal or doughnut shape with a cavity that exhibits a hydrophobic character, whereas the outside of the molecule is hydrophilic. With the aim of extending the physicochemical properties and inclusion capacity of natural CDs, various kinds of CD derivatives such as hydrophilic, hydrophobic, and ionic derivatives have been synthesized. Hydrophilic CDs can be used to improve the bioavailability of poorly water-soluble drugs in immediate release formulations. On the contrary, hydrophobic CDs can act as sustained-release carriers for water-soluble drugs. It is desirable for drug carriers to have certain properties such as controlled release, absorption enhancing ability, safety and quality, and cost performance; these requisites are fulfilled by the different CD derivatives that can modify the physicochemical and inclusion properties of the host molecules (3).

Randomly methylated and hydroxypropylated derivatives result from etherification at the hydroxyl groups of the glucose residues. This substitution gives rise to a solubility enhancement associated to the loss of intermolecular H bonds between adjacent glucose units and to the formation of a statistically substituted material that contains a mixture of isomeric components, which results in an amorphous product (4,5).

The crystalline state has an important effect on various pharmaceutical properties such as solubility, dissolution rate, and bioavailability of poorly soluble drugs (3), and therefore, the complexation with CDs can control solid-state properties of drugs. Amorphous and crystalline complexes obtained by diverse methods have been widely described in the literature together with their possible pharmaceutical applications (6–9). The complexes with natural CDs tend to crystallize into two principal types called cage and channel structures (Fig. 2), depending on the guest properties. In the cage

[1] Department of Chemistry and Soil Sciences, Physical-Chemistry, University of Navarra, C/Irunlarrea s/n., 31080 Pamplona, Navarra, Spain.
[2] To whom correspondence should be addressed. (e-mail: itzvelaz@unav.es)

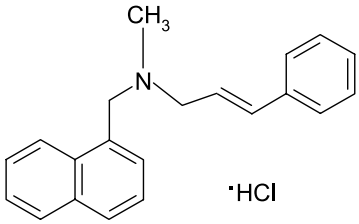

Fig. 1. Chemical structure of NF.

structure, both sides of the central cavity are blocked by other adjacent CD molecules forming isolated cages. Instead, the channel structures are formed by a sequence of dimer units of two neighboring CD molecules that are placed to form an endless column (7,10,11).

CDs can play a role in topical drug formulation with some possible application to the therapeutic use of NF (12). Several studies reveal the favorable influence of CD complexation in solid and semisolid formulations. It appears that CDs may improve dermal absorption of drugs mainly by increasing their thermodynamic activity in the vehicles and favoring their delivery to the skin surface (13–16). In this way, the incorporation of CD solid complexes to different topical formulations such as o/w cream formulations (12), microemulsions (17), hydroxypropyl methylcellulose gels (18), and liposomes (19) can improve the therapeutic effect of the drug, reduce its side effects, and enhance the drug dissolution, availability, diffusion properties, and permeation rate. In addition, it has been observed the usefulness of complexes with CDs for topical administration when a prolonged absorption in time is desired because CDs can act as a depot (20).

The aim of this paper is to study the interactions between NF and different CDs (α-CD, β-CD and derivatives, and γ-CD) in an aqueous medium and in the solid state. NF, being a weak base, is poorly soluble when it is found in the nonionized form, but it is probable that its complexation with CDs would be favored in such conditions. The low solubility of NF free base precludes the use of spectroscopic methods in studying its binding with CDs at pH 12, although it was possible to determine spectrophotometrically the stability constants of the ionized form in water (21).

The experiments in solution have been carried out by the solubility method to determine the binding constants of the complexes formed with the nonionized form. In addition, solid systems of NF and CD in a 1:1 molar ratio have been prepared and characterized to identify amorphous or crystalline structures and to differentiate between the cage and channel crystal types. The stability of the solid complexes has been studied, and preliminary dissolution rate assays with the NF–CD solid systems have been performed as well.

MATERIALS AND METHODS

Materials

Naftifine hydrochloride (molecular weight, 322.4) was kindly supplied by Schering (Milan, Italy). β-CD, Mβ-CD, and HPβ-CD were from Roquette S.A. (Lestrem, France), Cyclolab (Budapest, Hungary), and Sigma (Missouri, USA), respectively. Mβ-CD and HPβ-CD had average substitution degrees DS ≈ 12 and 4, respectively. γ-CD and α-CD were purchased from Wacker Chemie GmbH (Munich, Germany). All other reagents and solvents were from Panreac (Barcelona, Spain).

Methods

pH–Solubility Profile: Determination of pK_a

The solubility was determined by adding excess amounts of NF to different aqueous solutions ranging from pH 1.2 to 12.0. Depending on the desired pH value, the different aqueous solutions were prepared using the following reagents: HCl, Na_2HPO_4, KH_2PO_4, $NaHCO_3$, NaOH, and $KHC_8H_4O_4$.

The mixtures were shaken until equilibrium was reached. Then, the absorbance of filtered aliquots was measured at 254 nm. The pK_a value was obtained from the solubility–pH profile using the Henderson–Hasselbalch equation.

Solubility Studies

The solubility assays have been made in pH 12 aqueous solutions at 25°C. This buffer solution was prepared from Na_2HPO_4 (0.05 M) and NaOH (1 M) solutions.

The experiments were carried out by adding an excess of drug (15 mg) to 20-mL buffer solutions containing different concentrations of CD (1.0×10^{-3} to 2.0×10^{-2} M for α-CD, Mβ-CD, and HPβ-CD; 1.0×10^{-3} to 1.0×10^{-2} M for β-CD; 1.0×10^{-3} to 4.0×10^{-2} M for γ-CD). The test tubes were placed in a water bath at a constant temperature and shaken until equilibrium was reached (approximately 24 h). Then, the samples were filtered through a 0.45-μm cellulose filter, diluted, and measured at 222 nm with an HP8452A diode-array spectrophotometer. The molar absorptivity of NF was equal to 53.4×10^3 M^{-1} cm^{-1}. The presence of the ligands did not interfere with the absorption measurements at the experimental conditions. The assays were made in triplicate.

The apparent stability constants and the stoichiometry of complexes were estimated from the phase-solubility diagrams (22).

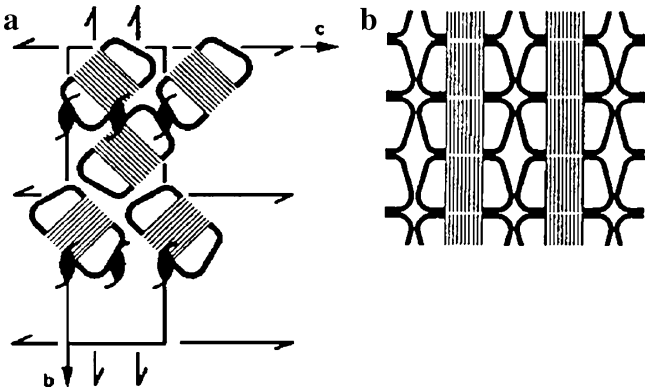

Fig. 2. Schematic description of (a) cage and (b) channel crystal structures formed by CD inclusion complexes. Taken from (10).

When a linear diagram is obtained (A_L), then the apparent stability constant (K_{11}) for the interaction can be calculated using:

$$S_t = S_o + \frac{K_{11}S_o[\mathrm{CD}]}{1 + K_{11}S_o} \quad (1)$$

where S_t and S_o are the molar solubility of the drug in presence and absence of CDs, respectively. K_{11} can be obtained from the slope of the straight line.

The stoichiometry with respect to the ligand (n) can be verified by:

$$\log\frac{S_t - S_o}{S_o} = \log K_{1n} + n\log[\mathrm{CD}] \quad (2)$$

If a nonlinear plot with concave-upward curvature (A_p type) is obtained, it means that at least one complex is present, having a stoichiometry >1 with respect to the ligand. The most probable case is that of 1:1 and 1:2 stoichiometries, and the following equation can be used to calculate the stability constants (K_{11} and K_{12}):

$$\frac{S_t - S_o}{[\mathrm{CD}]} = K_{11}S_o + K_{11}K_{12}S_o[\mathrm{CD}] \quad (3)$$

Another type of diagram is classified as B_S, and the isotherm presents a plateau in which the complex solubility is reached; the length of this plateau allows to calculate the stoichiometry of the complex, whereas the apparent stability constant can be obtained from the initial straight portion of the diagram using Eq. (1).

Solid Systems

Solid systems containing NF and the different CDs were prepared in a 1:1 molar ratio. The physical mixtures (PM) were prepared by a careful mixing with a microspatula for 15 min. The kneaded (KN) product was obtained by wetting the mixture of NF and CD with a minimum volume of a 50% v/v ethanol/water solution to obtain a paste, which was subsequently dried at room temperature. The coevaporated (CE) systems were prepared by mixing hydroalcoholic solutions (ethanol/water 50% v/v) of NF and the different CDs. These solutions were stirred, and the solvent was eliminated under vacuum in a rotatory evaporator at 85°C; the system was dried at room temperature.

The coprecipitated (CP) product for the NF–γ-CD system was obtained from the solid residue of the solubility assays. Complex formation can be observed in the precipitate from the end of the plateau to the final portion of the B_S solubility diagram (Fig. 4d).

Characterization of Solid Dispersions

X-ray powder diffraction patterns were collected on a Brucker D8 Advance diffractometer, with a $CuK_{\alpha 1}$ radiation, at a 40-kV voltage and a 30-mA current. The thermal analysis was performed with a simultaneous SDTA/TGA 851^e Mettler Toledo thermal analyzer. The thermal behavior was studied by heating about 15 mg of the sample at a scan rate of 5°C min^{-1} in a pierced aluminum crucible under static air atmosphere (25–450°C). The thermograms are shown from 25 to 200°C because it is the most interesting region. Infrared spectra were obtained with a Fourier transform infrared (FTIR) Nicolet Avatar 360 spectrophotometer with OMNIC ESP software, using the KBr pellet technique; the resolution was 2 cm^{-1}, and the spectra were the result of averaging 100 scans.

Dissolution Studies

Preliminary dissolution studies of pure NF and the NF–β-CD and NF–HPβ-CD CE and PM products have been performed taking 9 mg of NF or equivalent in powder into 25 mL of pH 7.0 ± 0.3 buffer phosphate as dissolution medium in sealed glass containers that were shaken at constant temperature (37 ± 0.5°C). Samples were taken at different times and filtered, and the NF concentration was spectrophotometrically determined at 254 nm. The variation in NF concentration due to the dilution caused by replacement of the samples volume with dissolution medium was corrected. Relative dissolution rates have been calculated as the ratio of the amount of drug dissolved at 350 min with respect to that obtained with the pure drug.

RESULTS AND DISCUSSION

pH–Solubility Profile: Determination of pK_a

The NF solubility as a function of pH can be observed in Fig. 3. The solubility value drastically decreases when the free base is formed. From these results, the pK_a value, determined by means of the Henderson–Hasselbalch equation, was 8.0 ± 0.2.

Solubility Diagrams

The phase-solubility diagrams obtained permit to study the binding between NF and different CDs (Fig. 4). From the intercept of the diagrams, the solubility of the pure drug has been determined equal to (4.6 ± 0.4) × 10^{-6} M.

In the case of α-CD, no change was observed in the solubility of NF, suggesting that NF does not fit in the α-CD cavity. In agreement with this result, molecular modeling studies on complexation with some benzene derivatives also show that the benzene ring is outside the α-CD cavity (23).

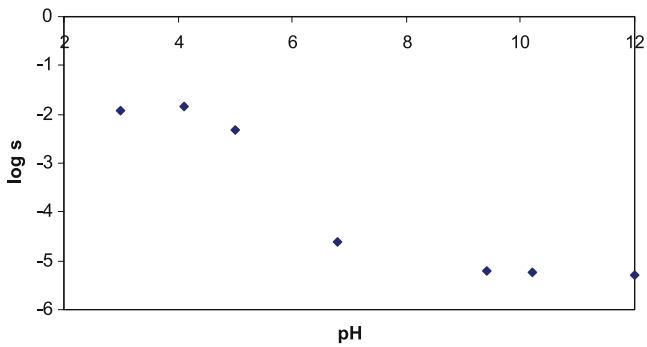

Fig. 3. pH–Solubility profile of NF.

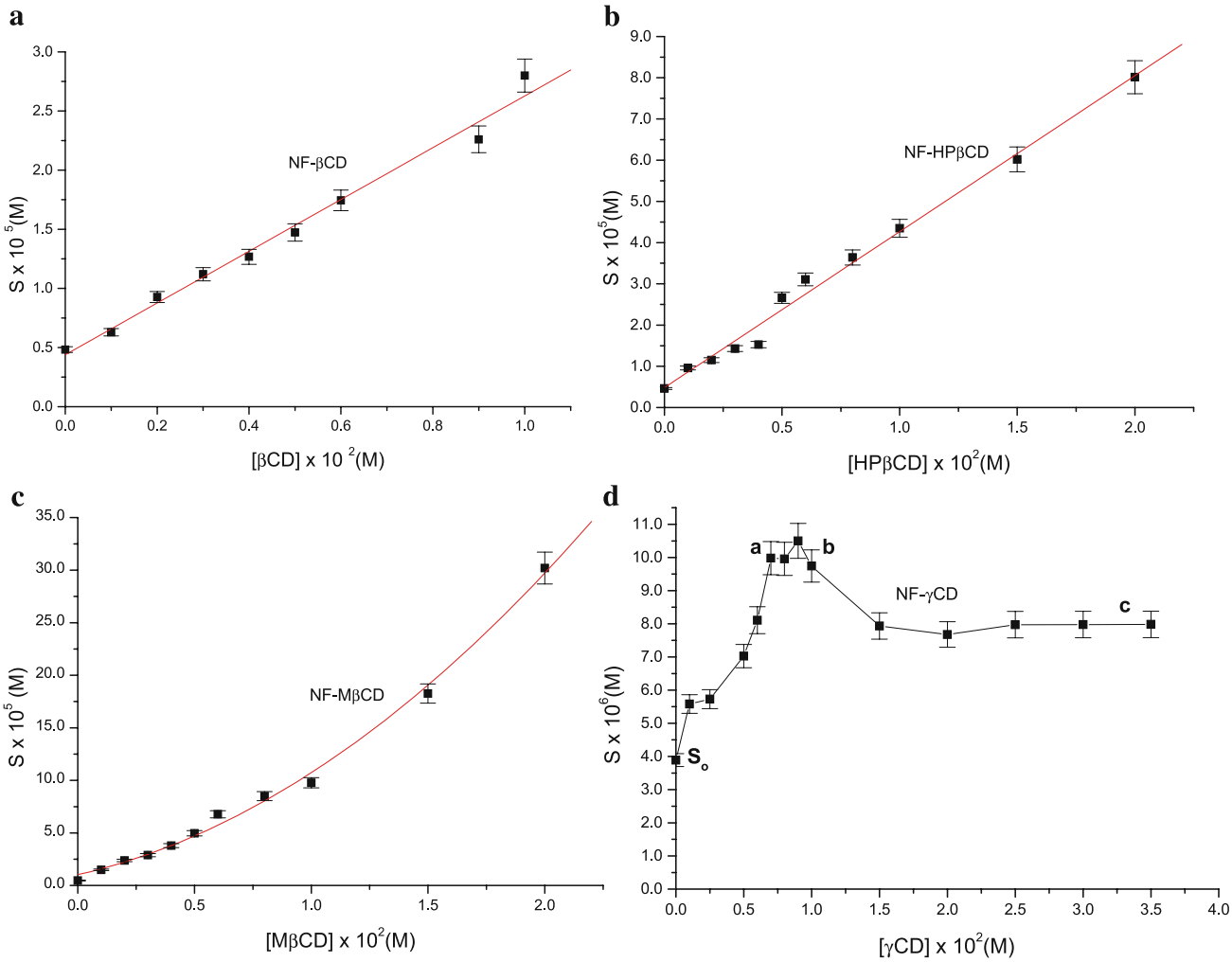

Fig. 4. Phase-solubility diagrams of NF–CD systems in pH 12 aqueous solution at 25°C.

An increase of 5-, 9-, and 21-fold in NF solubility is observed in presence of 1.0×10^{-2} M solutions of β-CD, HPβ-CD, and Mβ-CD, respectively, showing the influence of the CD rim characteristics on complex formation. Although β-CD is expected to provide a good fitting for the drug within the cavity, the solubility enhancement obtained is limited by the solubility of β-CD itself (24).

It has been observed that the solubility of the drug increases linearly as a function of β-CD and HPβ-CD concentration (A_L-type isotherm; Fig. 4a and b); this fact indicates that a hydrosoluble complex of probable 1:1 stoichiometry is formed. The stoichiometry with respect to CDs has been confirmed by Eq. (3); the resulting n values equal to 1.1 and 1.0 with β-CD and HPβ-CD, respectively. The apparent stability constants of the two complexes can be calculated by Eq. (1) and are shown in Table I. It can be concluded that the interaction between NF and HPβ-CD is stronger than that with β-CD. The substituent present in the CD rims plays an important role in determining the extent of complexation. The hydroxypropyl substitution induces changes in the hydrodynamic and hydrophobic interactions, which contribute to the complex stability (6). The higher complexing effectiveness of hydroxypropylated derivatives with respect to the natural CD can also be related to their higher aqueous solubility and to the hydrophobic cavity that is enlarged by the hydroxyalkyl groups on the CD rims (25).

Complexation with Mβ-CD gives rise to an A_p-type solubility diagram (Fig. 4c), which suggests that at least one complex of stoichiometry >1 with respect to the ligand could be formed. The apparent stability constants K_{11} and K_{12} can be calculated from Eq. (3) (Table I). The value of K_{12} is approximately 13-fold smaller than K_{11}, even though it is also possible that the solubilization of NF at high concentration of Mβ-CD is influenced by the surfactant effects of the latter (6).

The NF solubility increases only 2-fold in the presence of 1.0×10^{-2} M γ-CD. The phase-solubility diagram obtained for NF–γ-CD is of the B_S type, which corresponds to the

Table I. Apparent Stability Constants[a] for the Complexation of Naftifine with Different Cyclodextrins in pH 12 Aqueous Solution at 25°C

	β-CD	HPβ-CD	Mβ-CD	γ-CD
K_{11} (M^{-1})	512 ± 33	829 ± 22	1123 ± 29	184 ± 16
K_{12} (M^{-1})			89 ± 1	

[a] Values are the mean ± SE of three determinations.

formation of a complex of limited solubility (Fig. 4d). The molar ratio NF–γ-CD calculated for the binding is equal to 0.9, in agreement with 1:1 stoichiometry, and the apparent binding constant K_{11} is collected in Table I. The higher standard errors obtained for this diagram can be related to the low solubility of the NF–γ-CD complex.

The wide differences among the stability constants with each CD can allow to adjust the release of NF from the complexes in a particular vehicle. The highest stability constant is obtained for the NF–Mβ-CD system, probably due to the role of the methyl substituents in the hydrophobic interactions. The lowest value corresponds to the complex with γ-CD, which could be attributed to a less tight fitting of the drug within the cavity. The values of the stability constants obtained for the NF–CD complexes are suitable for possible pharmaceutical applications (7).

Solid Complexes

The possible complexation of NF with different CDs (α-CD, β-CD, HPβ-CD, Mβ-CD, and γ-CD) in the solid state has been studied by comparison of the KN, CE, and CP products with the corresponding PMs.

X-Ray Diffraction

The diffraction patterns of the solid systems are displayed in Fig. 5. It can be seen that those corresponding to the PMs are always a superimposition of both components.

The diffraction pattern of the NF–α-CD CE system is equivalent to that of the PM, showing the main peaks of the cage α-CD structure at 2θ = 12.1°, 14.3°, and 21.7° (26). On the other hand, the diffraction pattern of the NF–α-CD KN product exhibits the channel α-CD peak at 2θ = 13° with high intensity, but there are no changes either in the characteristic cage peak at 2θ = 21.7° or that corresponding to the channel type at 2θ = 20°, suggesting an intermediate structure in the KN solid (26). Likewise, the thermal analysis (Fig. 6) of the PMs and CE products show three endothermic peaks corresponding to three types of crystallization water molecules, as it has been reported for the cage packing type (11), whereas the differential thermal analysis (DTA) curve of the KN solid displays a specific arrangement of the water molecules in the crystals.

These detected differences can be attributed to two different types of crystals of pure α-CD; hence, complex formation can be rejected taking into account that the main peaks of free NF at 2θ = 6.7 and 20.1° have not changed; that the endothermic peak at 182°C, associated to the melting of NF, is always present (Fig. 6); and that the FTIR spectra of all NF solid systems with α-CD are equivalent (Fig. 7). Likewise, the X-ray diffraction patterns and the DTA curves of CE and KN products of pure α-CD present the same differences as those obtained from the NF–αCD CE and KN products. Even though the hydrated crystals of natural CDs usually adopt the cage structure, the amount of water in the crystallization process determines the structure of crystals (11,26,27).

In relation to complexation with β-CD, in the first instance, it has been checked that the DTA curves and the X-ray diffraction patterns remain unaltered after processing pure β-CD by kneading and coevaporation. The diffraction patterns of NF–β-CD CE and PM present several differences, mainly the disappearance of the peak of pure NF at 2θ = 6.7°, which is an evidence of complex formation. Moreover, the new reflections appeared especially at 2θ values between 6.0° and 20°, suggesting a new arrangement of the β-CD molecules in the crystalline complex in relation to the cage structure present in the PM. Unlike α-CD and γ-CD, there is no characteristic peak in the diffraction patterns of β-CD, which allows to distinguish between the cage and channel structures (11). In the channel inclusion complex formed by β-CD with polymers (28), the cage peak at 2θ = 12.5°, just like what occurred in the NF–β-CD complex, was not observed. A recent study of solid-state complexation points out the relevance of some changes that experience the small auxiliary peaks of β-CD around 2θ = 6.25° upon complexa-

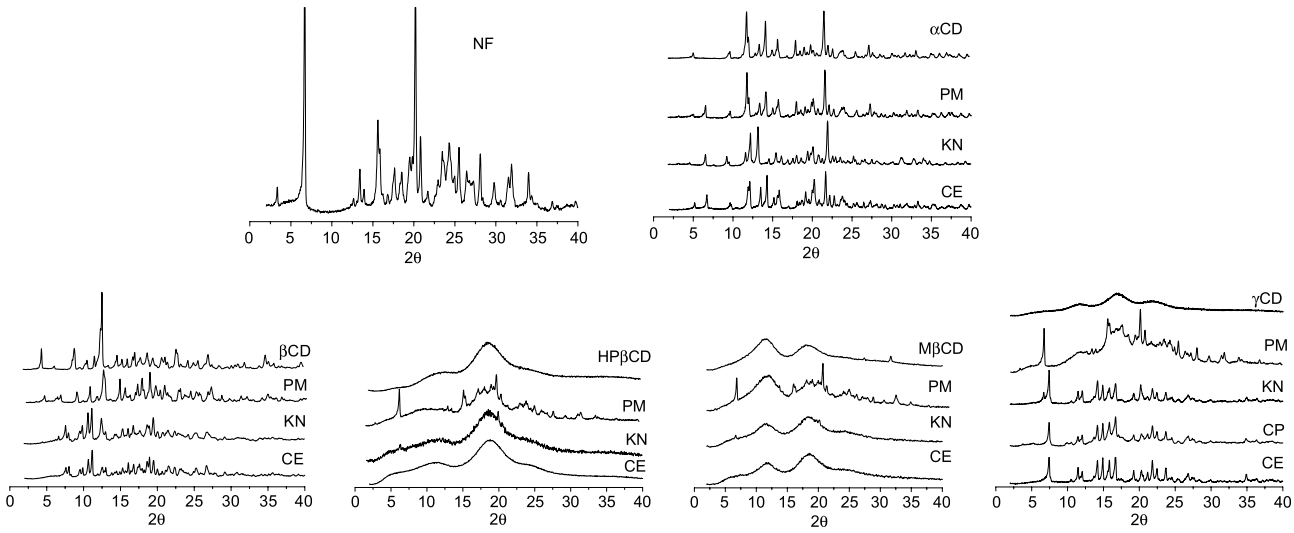

Fig. 5. X-ray diffraction patterns of single components and equimolar PM, CE, KN, and CP systems.

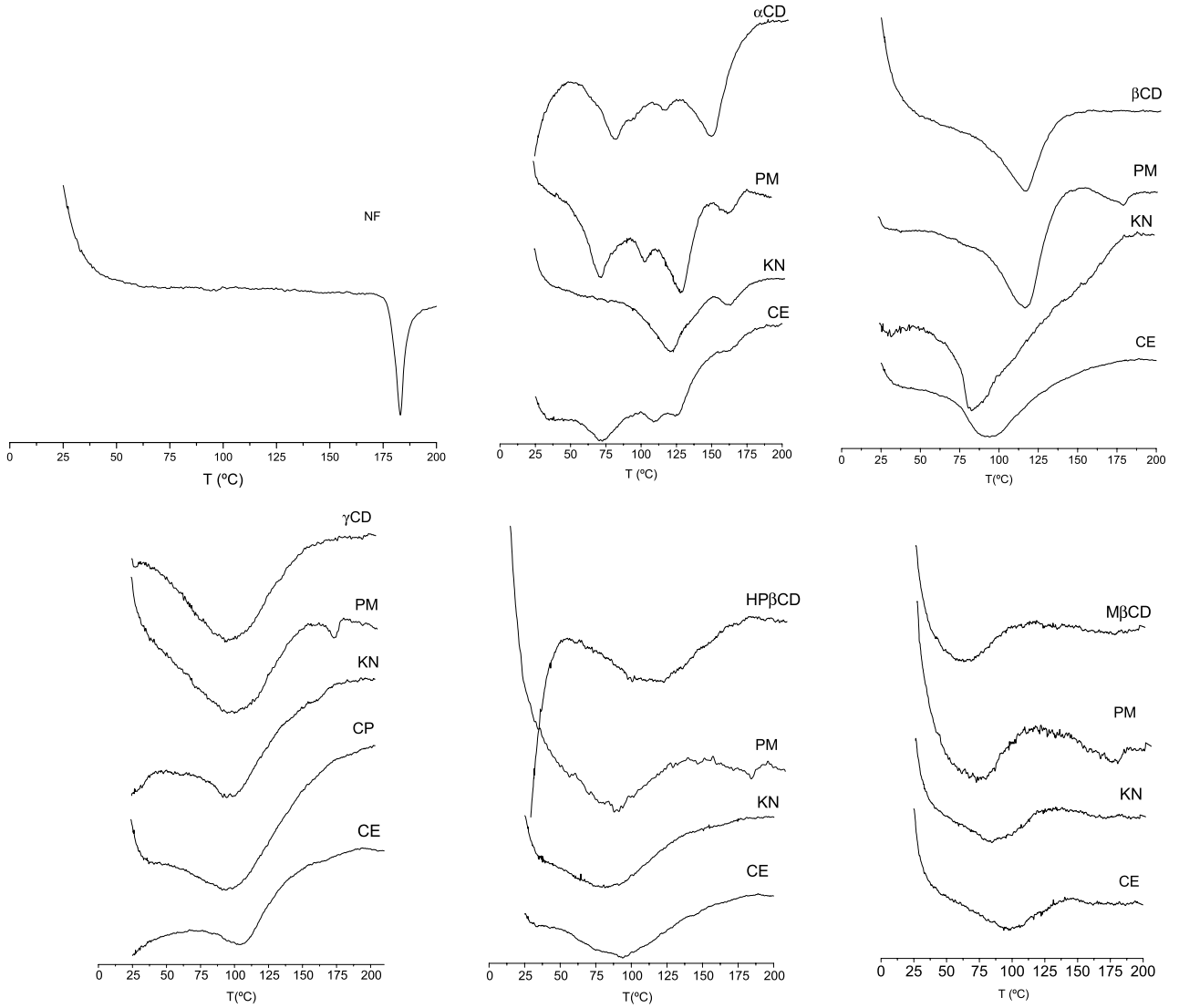

Fig. 6. Differential thermal analysis thermograms of NF, β-CD, HPβ-CD, Mβ-CD, and γ-CD, and their respective PM, CE, KN, and CP systems.

tion, which are related to variation of intermolecular distances within the crystal lattice (29). Our X-ray diffraction results appeared to display similar changes in the region of 2θ between 6° and 8°, but the intensity of the signals is low. Ghermani *et al.* (30) also suggested that certain changes in this region could be an evidence for complexation.

The diffraction pattern of the KN system shows the main reflections of the crystalline complex together with those of the PM; therefore, complex formation is not completed by kneading and depends on the mixing time.

It is noteworthy that β-CD is also able to form crystalline complexes with NF in the absence of solvent by simple and continuous grinding. For this reason, the mixing must be careful and time-limited when PMs are intended to be prepared.

The drying of the crystalline NF–β-CD complex at 70°C results in the formation of an amorphous complex whose X-ray diffraction diagram is similar to that of the complex anthracene–β-CD dried in vacuum at 80°C (31). Amorphous CD complexes can improve solid-state properties of drugs and are related with the loss of crystallization water molecules (10).

HPβ-CD and Mβ-CD, as well as their CE and KN products with NF, are amorphous; the peaks of the drug have almost disappeared in both systems but the disappearance was more complete in the CE solids. It could evidence the formation of amorphous complexes because the new interactions between NF and substituted CD prevent the crystallization of the free drug. The stability of the amorphous state of NF complexes with β-CDs has been verified in the course of 10 months, showing again that CDs are able to stabilize the amorphous state of some drugs (32).

On the other hand, although γ-CD is amorphous, the NF–γ-CD CE, KN, and CP products present similar diffraction patterns that differ significantly from that of the PM. The presence of new peaks of high intensity at 2θ = 7.5°, 11.4°, 14.2°, 16.7°, 21.8°, and 23.7°, together with the absence of the main reflections of pure NF, points out the formation of a new solid phase with high crystallinity. These new peaks are characteristic of hydrated complexes with γ-CD, in which

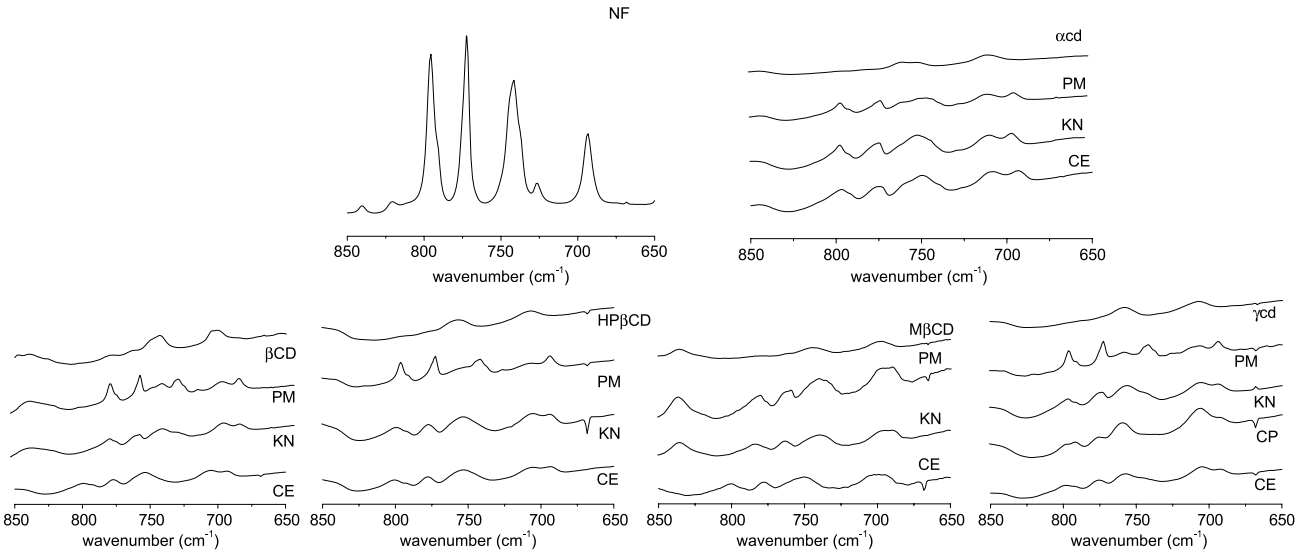

Fig. 7. Fourier transform infrared spectra of NF, β-CD, HPβ-CD, Mβ-CD, and γ-CD, and their respective PM, CE, KN, and CP systems.

the CD adopts the channel structure, irrespective of the guest properties (33); the peak at $2\theta = 7.6°$ has been proposed as an indicator for the γ-CD channel-type packing (11). Again, this result proves the inability of the cage structure of γ-CD to include the guest molecule because another adjacent γ-CD molecule is partially inserted in the cavity by the secondary hydroxyl side (7). The stability of the CD solid complexes depends on the hydration degree; in this sense, the NF–γ-CD complexes lose their crystalline structure when they are dried at 70°C, and their diffraction patterns become similar to those of the PM, displaying the main peaks of NF and the amorphous γ-CD state.

The amorphous state of γ-CD is related to the loss of less than half of its hydration water (11). The X-ray diffraction patterns of KN and CE pure γ-CD products exhibit a high crystallinity, showing a mixture of the cage, intermediate, and channel structures.

NF–γ-CD exhibits the lowest stability constant due to the γ-CD cavity size; on the other hand, NF shows remarkable ability for being included in the void of the columnar γ-CD structure by all the preparation methods tested: kneading, coevaporation from ethanol/water mixtures, and coprecipitation from pH 12 aqueous solution.

Finally, as it was mentioned above for the amorphous systems, the X-ray diffraction patterns of the crystalline complexes likewise did not change after 10 months of storage at room temperature.

Thermal Analysis

The DTA thermogram of NF shows a sharp endothermic peak at 182°C, which corresponds to the melting point of the drug (Fig. 6). The decomposition process happens in two steps with a total mass loss of 86%; it takes place between 210 and 440°C. The endothermic peak corresponding to the melting point of NF is detected in the PMs, but it disappears in the CE, KN, and CP systems. This thermal behavior can evidence the formation of complexes in the solid state between NF and the CDs studied, with the exception of α-CD. The decrease in the melting signal of NF in the PMs in relation to pure NF can be due to the interaction between both components induced by heating, especially with HPβ-CD and Mβ-CD (34).

The decomposition process of CD in the systems with NF occurs at a lower temperature than that of the pure CD. It starts at 200°C and finishes at 450°C in a single step.

The DTA curves shown in Fig. 6 exhibit the endothermic peaks corresponding to the loss of water from each system. The differences detected between the complexes and the PMs, mainly for the NF–β-CD system, also indicate a

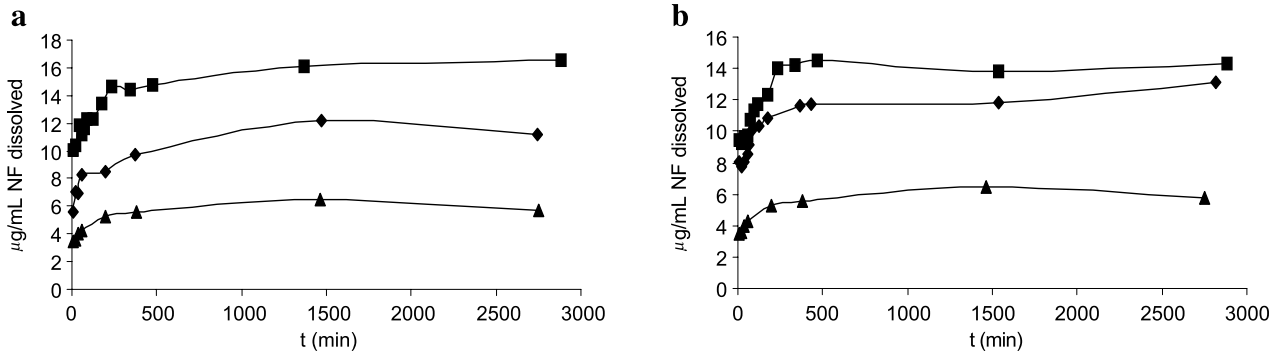

Fig. 8. Dissolution curves of NF alone (▲) and NF–β-CD (A) and NF–HPβ-CD (B) equimolar systems: PMs (♦) and CE products (■).

phase transition in the CD structure during complexation. The temperature of water loss changes from 120°C in the PM to 90°C in the NF–β-CD crystalline complex. The numbers of water molecules per CD unit in the complexes with β-CD, HPβ-CD, Mβ-CD, and γ-CD have been determined to be 9, 5, 3, and 10, respectively.

FTIR Spectroscopy

The changes between the FTIR spectra of free and complexed NF are more obvious in the region of 825–700 cm^{-1} for all the CDs, except for α-CD (Fig. 7). The band at 772 cm^{-1} corresponds to the bending vibration of the aromatic C–H bond (35). This band appears unchanged in the PM, but it broadens and shifts to a higher frequency in the CE and KN products; this fact points out the inclusion of the aromatic rings into the CD cavity. The spectrum of the CP system formed from NF and γ-CD aqueous solutions corresponds to that of the CE solid and shows the complex characteristic bands.

Dissolution Rate

As it has been observed, complexation with CDs improves the solubility of the drug in alkaline media, but it is also interesting to study the effect of solid-state complexation on the dissolution rate of the drug. Therefore, preliminary studies have been performed to obtain the dissolution profiles of pure NF, NF–βCD, and NF–HPβCD CE and PM products at pH 7.0 ± 0.3 and 37 ± 0.5°C.

The experimental results of the dissolution studies are shown in Fig. 8. It can be observed that both complexes and PMs exhibited faster dissolution rates than that of pure NF. The relative dissolution rates at 350 min were found to be 1.7 and 2.6 for NF–β-CD PM and CE products, respectively, and the values for the same solid systems of NF with HPβ-CD were 2.1 and 2.5, respectively.

The improvement on the dissolution rate of PMs in comparison with NF alone can be due to a solubilizing action of β-CD and HPβ-CD, as their hydrophilic effect can reduce the interfacial tension between NF and the dissolution medium, improve drug wettability, and form readily soluble complexes in the dissolution medium (36).

A similar trend was found with natural β-CD and HPβ-CD complexes, and no significant difference was found between these two carriers. Moreover, it can be observed that the CE products are more efficient than the PMs. It could be due to a closer contact between NF and the CD, with a better molecular dispersion of the drug into the hydrophilic carrier, together with the interaction that occurs in the solid state (34,37). Finally, the dissolution profile of the NF–β-CD KN product (not shown) was similar to that of the CE product, as expected from the solid-state studies (38).

ACKNOWLEDGMENT

The authors gratefully acknowledge the financial support provided by the Comisión Interministerial de Ciencia y Tecnología (Project MAT2003-08390-C02-01).

REFERENCES

1. N. S. Ryder and M.-C. Dupont. Inhibition of squalene epoxidase by allylamine antimycotic compounds. *Biochem. J.* **230**:765–770 (1985).
2. A. Stütz, A. Georgepoulos, W. Granitzer, G. Petrany, and D. Berney. Synthesis and structure–activity relationships of naftifine-related allylamine antimycotics. *J. Med. Chem.* **29**:112–125 (1986).
3. K. Uekama. Design and evaluation of cyclodextrin-based drug formulation. *Chem. Pharm. Bull.* **52**(8):900–915 (2004).
4. K.-H. Frömming and J. Szejtli. *Cyclodextrins in Pharmacy*. Kluwer Academic Publishers, The Netherlands, 1994.
5. M. E. Davis and M. Brewster. Cyclodextrin-based pharmaceutics: past, present and future. *Nat. Rev., Drug Discov.* **3**: 1023–1035 (2004).
6. D. Duchêne. *New Trends in Cyclodextrins and Derivatives*. Editions De Santé, Paris, 1991.
7. J. Szejtli and T. Osa. *Comprehensive Supramolecular Chemistry: Cyclodextrins,* Vol. 3 Elsevier, UK, 1996.
8. A. R. Hedges. Industrial applications of cyclodextrins. *Chem. Rev.* **98**:2035–2044 (1998).
9. E. M. Martín del Valle. Cyclodextrins and their uses: a review. *Process Biochem.* **39**:1033–1046 (2004).
10. W. Saenger, J. Jacob, K. Gessler, T. Steiner, D. Hoffmann, H. Sanbe, K. Koizumi, S. H. Smith, and T. Takaha. Structures of the common cyclodextrins and their larger analogues beyond the doughnut. *Chem. Rev.* **98**:1787–1802 (1998).
11. C. C. Rusa, T. A. Bullions, J. Fox, F. E. Porbeni, X. Wang, and A. E. Tonelli. Inclusion compound formation with a new columnar cyclodextrin host. *Langmuir* **18**:10016–10023 (2002).
12. T. Loftsson and M. Masson. Cyclodextrins in topical drug formulations: theory and practice. *Int. J. Pharm.* **225**:15–30 (2001).
13. T. Loftsson, M. Masson, H. H. Sigurdsson, P. Magmusson, and F. Legoffic. Cyclodextrins as co-enhancers in dermal and transdermal drug delivery. *Pharmazie* **53**:137–139 (1998).
14. H. Matsuda and H. Arima. Cyclodextrin in transdermal and rectal delivery. *Adv. Drug Deliv. Rev.* **36**:81–99 (1999).
15. M. Masson, T. Loftsson, G. Masson, and E. Stefansson. Cyclodextrins as permeation enhancers: some theoretical evaluations and *in vitro* testing. *J. Control. Release* **59**:107–118 (1999).
16. J. Manosroi, M. G. Apriyani, K. Foe, and A. Manosroi. Enhancement of the release of azelaic acid through the synthetic membranes by inclusion complex formation with hydroxypropyl-β-cyclodextrin. *Int. J. Pharm.* **293**:235–240 (2005).
17. M. E. Dalmora, S. L. Dalmora, and A. G. Oliveira. Inclusion complex of piroxicam with β-cyclodextrin and incorporation in cationic microemulsion. *In vitro* drug release and *in vivo* topical anti-inflammatory effect. *Int. J. Pharm.* **222**:45–55 (2001).
18. M. Jug, M. Becirevic-Lacán, A. Kwokal, and B. Cetina-Cizmek. Influence of cyclodextrin complexation on piroxicam gel formulations. *Acta Pharm.* **55**(3):223–236 (2005).
19. F. Maestrelli, M. L. González-Rodríguez, A. M. Rabasco, and P. Mura. Preparation and characterisation of liposomes encapsulating ketoprofen–cyclodextrin complexes for transdermal drug delivery. *Int. J. Pharm.* **298**:55–67 (2005).
20. E. Larrucea, A. Arellano, S. Santoyo, and P. Ygartua. Combined effect of oleic acid and propylene glycol on the percutaneous penetration of tenoxicam and its retention in the skin. *Eur. J. Pharm. Biopharm.* **52**(2):113–119 (2001).
21. M. Uzqueda, M. Sánchez, I. Vélaz, C. Martín, A. Zornoza, and C. Martínez-Ohárriz. *Spectrophotometric study of the interactions between naftifine and cyclodextrins. 12th European Carbohydrate Symposium (Eurocarb 12). Book of Abstracts*. Grenoble, France, 2003, p. 182.
22. K. A. Connors. *Binding Constants: The Measurement of Molecular Complex Stability,* Chapter 8. Wiley, USA, 1987.
23. E. Estrada, I. Perdomo-López, and J. J. Torres-Labandeira. Combination of 2D-, 3D-connectivity and quantum chemical descriptors in QSPR. Complexation of α- and β-cyclodextrin with benzene derivatives. *J. Chem. Inf. Comput. Sci.* **41**(6):1561–1568 (2001).

24. N. Nasongkla, A. F. Wiedmann, A. Bruening, M. Beman, D. Ray, W. G. Bornmann, D. A. Boothman, and J. Gao. Enhancement of solubility and bioavailability of β-lapachone using cyclodextrin inclusion complexes. *Pharm. Res.* **20**(10):1626–1633 (2003).
25. M. D. Veiga, M. Merino, M. Cirri, F. Maestrelli, and P. Mura. Comparative study on triclosan interactions in solution and in the solid state with natural and chemically modified cyclodextrins. *J. Incl. Phenom. Macrocycl. Chem.* **53**:77–83 (2005).
26. M. A. Hunt, C. C. Rusa, A. E. Tonelli, and C. M. Balik. Structure and stability of columnar cyclomaltohexaose (α-cyclodextrin) hydrate. *Carbohydr. Res.* **339**:2805–2810 (2004).
27. M. A. Hunt, C. C. Rusa, A. E. Tonelli, and C. M. Balik. Structure and stability of columnar cyclomaltooctaose (γ-cyclodextrin) hydrate. *Carbohydr. Res.* **340**:1631–1637 (2005).
28. J. Li, B. Chen, X. Wang, and S. H. Goh. Preparation and characterization of inclusion complexes formed by biodegradable poly(ε-caprolactone)–poly(tetrahydrofuran)–poly(ε-caprolactone) triblock copolymer and cyclodextrins. *Polymer* **45**:1777–1785 (2004).
29. D. Bongiorno, L. Ceraulo, M. Ferrugia, F. Filizzola, A. Ruggirello, and V. T. Liveri. Inclusion complexes of cyclomaltooligosaccharides (cyclodextrins) with melatonin in solid phase. *Arkivoc* **14**:118–130 (2005).
30. N. E. Ghermani, A. S. Biré, N. Bouhmaida, S. Ouharzoune, J. Bouligand, A. Layre, R. Gref, and P. Couvreur. Molecular reactivity of busulfan through its experimental electrostatic properties in the solid state. *Pharm. Res.* **21**(4):598–604 (2004).
31. K. Takeo and T. Kuge. Complexes of starchy materials with organic compounds. Part III. X-ray studies on amylose and cyclodextrin complexes. *Agric. Biol. Chem.* **33**(8):1174–1180 (1969).
32. M. Cirri, F. Maestrelli, S. Furlanetto, and P. Mura. Solid-state characterization of glyburide-cyclodextrin co-ground products. *J. Therm. Anal. Calorim.* **77**:413–422 (2004).
33. K. Takeo and T. Kuge. Complexes of starchy materials with organic compounds. Part IV. X-ray diffraction of γ-cyclodextrin complexes. *Agric. Biol. Chem.* **34**(4):568–574 (1970).
34. B. Capello, C. Di Maio, and M. Iervolino. Investigation on the interaction of bendazac with β-, hydroxypropyl-β- and γ-cyclodextrins. *J. Incl. Phenom. Macrocycl. Chem.* **43**:251–257 (2002).
35. I. Alberti, Y. N. Kalia, A. Naik, J. D. Bonny, and R. H. Guy. *In vivo* assessment of enhanced topical delivery of terbinafine to human stratum corneum. *J. Control. Release* **71**:319–327 (2001).
36. L.-P. Ruan, B.-Y. Yu, G.-M. Fu, and D. Zhu. Improving the solubility of ampelopsin by solid dispersions and inclusion complexes. *J. Pharm. Biomed. Anal.* **38**:457–464 (2005).
37. P. Mura, N. Zerrouk, N. Mennini, F. Maestrelli, and C. Chemtob. Development and characterization of naproxen–chitosan solid systems with improved drug dissolution properties. *Eur. J. Pharm. Sci.* **19**(1):67–75 (2003).
38. G. Zingone and F. Rubessa. Preformulation study of the inclusion complex warfarin-β-cyclodextrin. *Int. J. Pharm.* **291**:3–10 (2005).